Maejo International Journal of
Energy and Environmental Communication

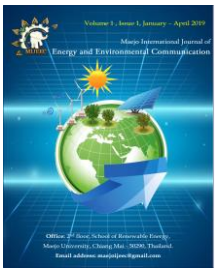

ARTICLE

Experimental study on liquid spray and small droplet formation in ethanol-oil system in a DC electric field

Dongbao Wang, Junfeng Wang*, Piyaphong Yongphet

School of Energy and Power Engineering, Jiangsu University, Zhenjiang, 212013, China

*Corresponding author, *E-mail address*: wangjunfeng@ujs.edu.cn

ARTICLE INFOR

Received 28th April 2019

Accepted 30th May 2019

Keywords:
Liquid spray
Electrostatic field
Spray mode
Droplet breakup
Liquid jet

ABSTRACT

A detailed experimental study on the evolution process of charged liquid deformation and breakup in another immiscible liquid from a capillary channel was conducted at micro-scale. By means of high-speed microscopy technique, various liquid spray modes and droplet formation processes were illustrated in detail at different flow rates and voltages. The effects of Reynolds (Re) and electric Bond (Bo_E) number on droplet size distribution were analyzed. It was found that droplet sizes rose with increasing Re while declined with increasing Bo_E. The experimental results show that electric field could promote interfacial area through decreasing interfacial tension to augment mass transfer between immiscible liquids at low flow rates. Besides, liquid spray experienced drip, deformation, breakup and jet modes with the increase of flow rate and electric potential. A critical Re of 170 was obtained beyond which electric field had little effect on liquid dynamic behaviors.

1. Introduction

Liquid dispersed into another immiscible fluid find many applications in the industrial process, such as emulsification and extraction. The increase of interfacial area is essential for components exchange among phases during these processes. It's known that small droplet size distribution of dispersed phase could promote mass transfer rates between two phases due to large interfacial area (Eastwood et al., 2004). Traditional methods of agitation and high pressure mixture are usually high energy consumption, which has driven the need for developing novel and effective technological approaches. Novel method such as electric field is regarded to be promising technologies that could play an important role in liquid dispersion to augment interfacial heat and mass transfer (Seyed-Yagoobi and Bryan, 1999). It is known that liquid droplet subjected to an external electric field could accumulate electric charges on its surface due to the conductivity of the liquid and the droplet would deform and breakup into small droplets when the total charges on the droplet surface reaches Rayleigh limit (Rayleigh, 1882). An experimental investigation on the charge and breakup of heptane droplets generated by electro spray dispersion with flash shadowgraph techniques has been reported based on Rayleigh's theory, and droplets could split at the sub-Rayleigh limit (Gomez and Tang, 1994). Thus, liquid under electric field could deform and disintegrate into small droplets, forming uniform droplet size distribution and large interfacial area between immiscible liquids.

In addition, the different dielectric properties could cause electrical stresses on the interface when a fluid droplet is injected into another liquid in the presence of an external electric field, which also results in droplet deformation and breakup for the decrease of interfacial tension. Coulombic or polarization forces induced by electric potential could be strong enough to influence the liquid dynamics so as to significantly modify heat and mass transport properties to strengthen blending process between immiscible fluids. Both normal and tangential stresses are exerted on droplet surface with the effect of electric field, leading to shape imbalance and droplet breakup. Allan and Mason (1962) conducted experiments in 1962 with a wide range of fluid systems, showing that droplets in electric field could deform into either prolate or oblate shape. Furthermore, fluid motion inside and outside the droplet known electrohydrodynamic (EHD) flow could be formed to make electrical and hydrodynamic shear stresses at equilibrium, which could also be considered as a technology to augment two-phase heat and mass transfer (Seyed-Yagoobi and Bryan, 1999). Based on this, Taylor (1966) developed a theory known as leaky dielectric theory to justify the experimental results about electrohydrodynamic deformation of a droplet. Despite some discrepancy, following studies had proved the leaky dielectric theory to be correct for analyzing the flow and deformation pattern when no net charge exists on the droplet surface (Vizika and Saville, 1992; Feng and Scott, 1996; Reddy and Esmaeeli, 2009). Many literatures have discussed the charged single droplet deformation and breakup processes influenced by physical properties such as electrical conductivity, viscosity, surface tension and density, which is still ongoing (Jong-Wook and Seung-Man, 2000; Matsuyama, et al., 2007; Ristenpart et al., 2009; Jalaal et al., 2010; Raisin et al., 2011, Li et al., 2011).

However, droplet deformation and break-up process in electric field are very complex owing to many interfering parameters. The whole evolution process and morphology need to be captured so as to analyze the microscopic time-resolved and space-resolved dynamics behaviors by visualization technology of high-speed microscopy. The deformation and departure of bubbles attached to a wall were studied by Kweon et al. (1998) using visualization method. Electrospray system of liquid in air also takes advantage of visualization technology to study electrospray regimes (Marginean et al., 2006), spray dynamics (Nemes et al., 2007) and structures (Kim et al., 2011) as well as micro-jet breakup (Wang et al., 2012) and EHD characteristics (Min et al., 2013). Those studies have classified various breakup regimes such as dripping mode, spindle mode and whipping mode in electrospray (Marginean et al., 2006) and dripping mode, mixed mode and spray mode in air-water system (Won-Tae and Sotira, 1997). Although some works (Eow et al., 2003; Petera et al., 2005; Salipante and Vlahovska, 2010) have focused on single droplet deformation in liquid phase, a comprehensive understanding of visualization studies on the dynamic behavior of continuous injected dispersed liquid breakup is still in need.

The subject of the present work mainly concerns the dynamic evolution process of the charged liquid spray and droplet formation behaviors in immiscible liquid phase. With the presence of an external electric field, droplet deformation and breakup morphology were visualized while detailed droplet formation process was illustrated. In addition, the dripping droplet was found to turn into jet with the increase of flow rate but the increase of voltage couldn't strongly influence liquid jet behaviors at higher flow rates. Our study aims to provide some novel and special charged droplet behaviors for a better understanding of liquid-liquid dispersion mechanism in the presence of electric field.

Nomenclature and Abbreviation

Re	Reynolds
BoE	Electric bond
PTFE	Polytetrafluoroethylene
RSP01-B	Micro-flow digital pump
EHD	Electrohydrodynamic

2. Materials and methods

The experimental investigation mainly consists of charging facility, droplet formation devices and visualization system, which has been applied in the referenced papers (Wang, D et al. 2019a and 2019b). The detailed schematic diagram of the microscopic Perspex test-cell is illustrated in Figure 1. The droplet charging facility is carried out by utilization of a point-plane configuration charging device, which could charge the dispersed phase through a stainless steel plain-orifice capillary with inner and outer diameters of 400 μm and 710 μm. Supplied by a high-voltage DC generator (*negative, voltage 0-30kv, current 0-2.0 mA*), the electric charges are applied to the vertically mounted capillary by electric wires. A horizontal electrode of copper plate is mounted vertically over the capillary and electrically grounded. Distance H between the nozzle tip and grounded electrode is set to be 65 *mm*. To ensure safety and accuracy, all the other devices and components used in this experiment are insulated with polytetrafluoroethylene (*PTFE*) and electrically grounded. The micro-flow digital pump (*RSP01-B*) is used to supply liquid and control flow rate in the needle precisely. Two immiscible experimental media of ethanol and soybean oil that could be used to produce biodiesel are employed in current experiment. Their physical properties are shown in table 1. The dynamic behaviors of charged liquid breakup inception and evolution processes are observed and recorded by utilization of a high speed digital camera (*Phantom V1611*) with capacity of 10^5 frames per second (*fps*), using a microscopic zoom lens (Model *NAVITAR12X,* 12 times

magnified). A continuous light (*LED cold point light source*) with high frequency is placed against the lens of high-speed camera to illuminate the whole liquid breakup process. The liquid evolution process is recorded by high-speed camera at 5000 *fps*.

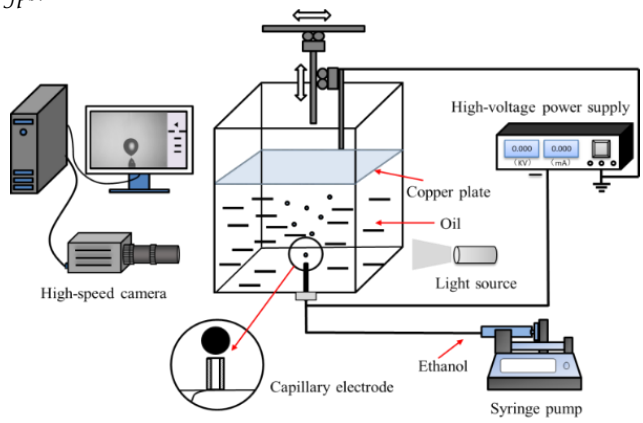

Figure1. Schematic of the experimental setup

The ethanol breakup evolution process in soybean oil phase is investigated under electric field with various flow rates. And the experiment is divided into two stages according to the inception of liquid form based on the amount of ethanol flow rates. At small flow rates from 0.001 *ml/s* to 0.01 *ml/s*, the ethanol liquid forms a series of single droplets from outlet of stainless needle. With the increase of ethanol flow rates from 0.02 *ml/s* to 0.2 *ml/s*, single ethanol droplet transits to liquid jet.

Table 1. The properties of liquids used in this experiment.

Medium	Density (kg/m^3)	Viscosity ($10^{-6}m^2/s$)	Surface tension (N/m)	Conductivity (S/m)
Soybean oil	915	54.74	0.032	0.1×10^{-5}
Ethanol	790	1.07	0.021	5.1×10^{-5}

3. Results and Discussion

3.1. Dynamic behaviors of dripping droplet formation at small flow rates

For small flow rates, the inception shape from nozzle tip is a single sphere droplet along the nozzle axial without exerting electric potential, which could be named as single droplet regime (Wang et al., 2019 a). The flow rate could be represented by Reynolds number *Re* and is about 2 for the smallest flow rate of 0.001 *ml/s*. The largest flow rate to produce single droplet is assumed to be 0.01 *ml/s* with *Re* of 22 in this experiment. With the rise of electric field strength *E*, single droplet regime disappears while other special breakup regimes could be found. Dimensionless *Re* could be derived from Eq. (1)

$$\mathrm{Re}=\frac{4\rho Q}{\pi\mu d_i} \tag{1}$$

Where ρ and μ are the density and viscosity of ethanol, respectively, Q represents the volume flow rate of ethanol liquid, and d_i is the inner diameter of nozzle.

In this dispersion stage, the charged droplet deformation resulting from the relative strength of electrostatic and capillary forces can be expressed by the electric Bond number (Reznik et al., 2004)

$$Bo_E=\frac{\varepsilon r E_0^2}{\lambda} \tag{2}$$

Where ε and λ are the soybean oil dielectric constant and the interfacial tension of two liquids, respectively, and E_0 represents the electric field strength at the capillary tip. For the point-plane arrangement used in the experiment, the electric field strength at the nozzle tip can be described by Coelho and Debeau (1971)

$$E_0=\frac{V}{r\ln\sqrt{\frac{4H}{r}}} \tag{3}$$

Where H is the distance between the nozzle tip and the copper plane electrode surface, r is the nozzle outer radius. The electric Bond number given by Eq. (2) could be then written as a function of the applied potential:

$$Bo_E=\frac{\varepsilon V^2}{\lambda r\left(\ln\sqrt{\frac{4H}{r}}\right)^2} \tag{4}$$

The electric Bond number is more accurate to identify liquid breakup regime transitions than a single voltage parameter, giving more sense to analyze the dynamics of charged droplet deformation and breakup process.

The initial ethanol evolution process is in the form of single sphere droplet at small Re as shown in Figure 2, producing a liquid bridge along the needle axis. In this regime, ethanol droplet is formed at a certain interval with stable size. It can be seen that the time scale for a whole dynamic behavior process is about 2.4 *s*. When electric potential is exerted on the droplet, the spherical droplet detaches from the nozzle tip due to buoyancy and electric forces against interfacial tension stresses, followed by a satellite droplet.

With the slight increase of electric potential, the droplet sizes become smaller while droplet formation frequency rises

due to electric force increase. By analyzing the captured images in a single breakup regime, the droplet size distribution and formation frequency are obtained at $Re = 2$ with various Bo_E. The mean diameters and frequency are

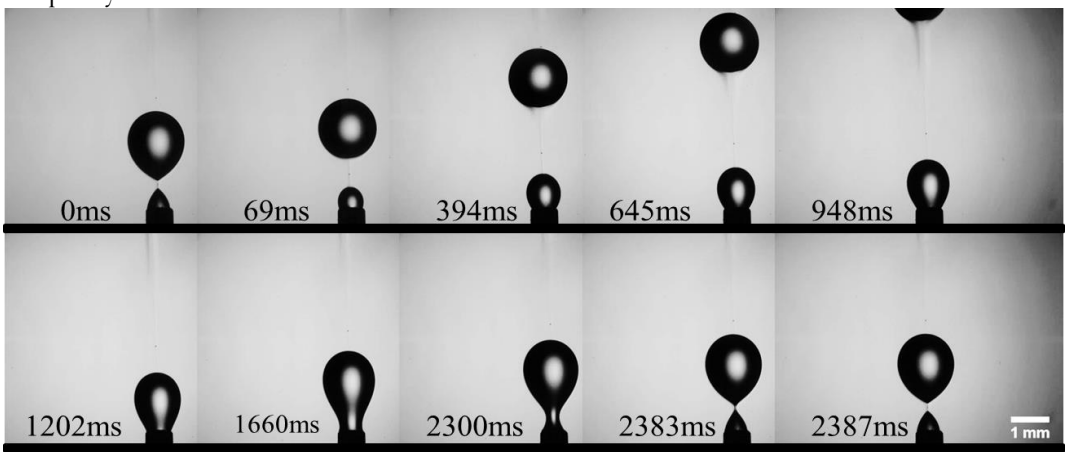

Figure 2. Dripping droplet of ethanol in soybean oil

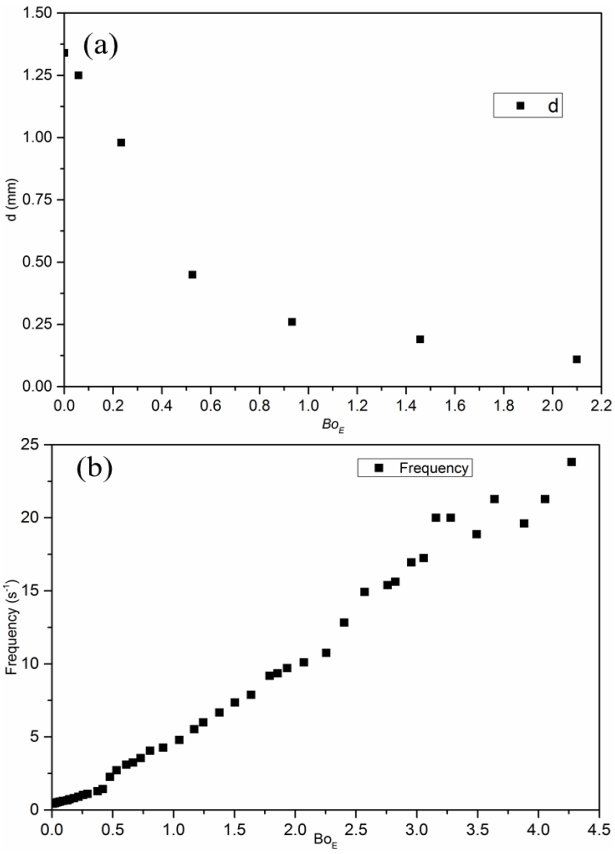

Figure 3. Droplet size distribution (a) and droplet formation frequency (b), Re = 2

given in Figure 3 (a) and (b), respectively. It can be seen that the droplet size decreases sharply with slight rise of Bo_E while formation frequency increase almost linearly, which means that more small droplets are produced so as to promote interfacial contact area. At $Re = 2$, the applied electric Bo_E increases from 0 to 2 with the droplet size declines from 1.3 mm to 0.1 mm, 13 times smaller than initial sizes. At the same time, 10 times of droplet amount are formed owing to the increase of frequency.

When flow rate increases at small scale, the droplet dynamic behaviors are similar to the above droplet formation cycle. The droplet diameter could be written as, $d = 2 * \sqrt[3]{\frac{3Q}{4\pi}}$ assuming that droplet shape is sphere.

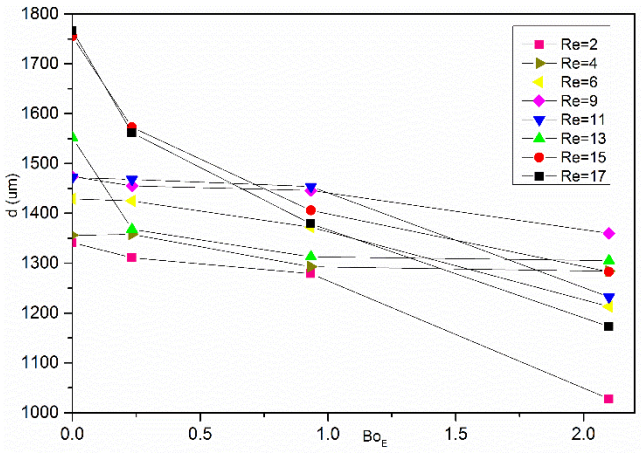

Figure 4. Droplet size distribution with various Re and Bo_E

Due to more liquid accumulation, the single droplet size becomes larger. However, electric force decreases surface tension so that droplet size decreases as the rise of electrical potential. These trends are described in Figure 4. With the Re increases from 2 to 17, the droplet size increases from 1350 μm to 1750 μm with no exerting potential. In addition, the droplet sizes show a declining trend with the increase of Bo_E regardless of flow rates. With the increase of

applied potential, droplet will experience deformation. The droplet departs from the nozzle axial, deviating and deforming at the vicinity of nozzle axial, which could be regarded as swing breakup regime as given by Figure 5 (Wang et al., 2019 a). The droplets deviate along the nozzle axial with smaller sizes as the increase of electric field while the droplet production frequency speeds up, forming two droplet arrays. In swing breakup regime, some spherical droplets deform to threads and the angle between two droplet arrays becomes larger with increasing Bo_E.

3.2. Dynamic behaviors of charged droplet breakup at small flow rates

When total charges on the droplet surface reach Rayleigh limits (Rayleigh, 1882), the inception of droplet breakup becomes violently, forming a branch-like shape and at the apex of each branch, several micro filament jets are formed from the liquid bridge, producing fine droplets. This dynamic behavior is named as branch breakup regime illustrated in Figure 6 (Wang et al., 2019 a). At the apex of each branch, the liquid filament tapers and deforms into about 3 filaments, the filament deforms, tapers and stretches into small liquid filament jets, producing more fine scale branches. Finally, much fine droplets eject from the micro jets. With the ejection of micro jets, the meniscus liquid bridges break off from the main trunk, producing some larger scale droplets.

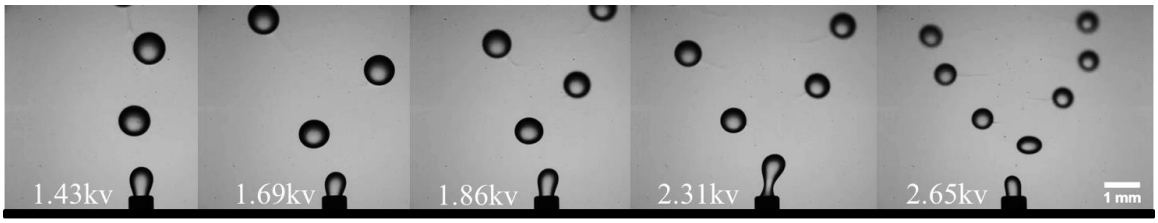

Figure 5. Swing breakup regime from inception to fully developed

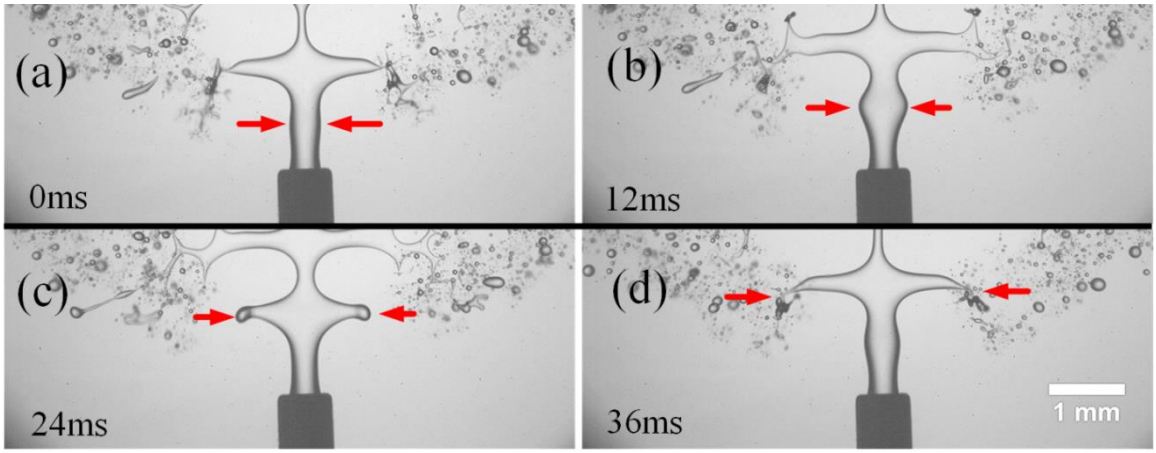

Figure 6. Branch breakup and tip spray

With much higher applied potential, the liquid bridge is stretched to grow into expanded thin sheet, while much more micro jets eject micron scale even nano scale droplets, this phenomenon is named as sheet breakup regime given by Figure 7 (Wang, D. et al, 2019a). Figure 7 (a) illustrates the transition from branch breakup regime to sheet breakup regime, where liquid bridges and main trunk are stretched and flattened to be thin sheet by electric force. Besides, the ligaments grow into fine jets on the edge of thin sheet, producing much fine and uniform droplets. What's more, the liquid bridges and trunk could be further flattened while tapering ligaments produce uniform droplet size distribution as given by Figure7 (b). What needs to be pointed out is that a special sheet breakup characteristic is captured, where the liquid sheet forms a candle-flame like shapes with fine jets standing on the edges, as shown in Figure 7 (c) and (d). In the titled flame sheet, the flow field turns to be uniform and the fine droplets of micron scale dispersed into oil phase. This sheet phenomenon is usually reported in impinging jets experiments (Swarup et al., 2017), where two high speed jets impinge and merge together to produce a rim sheet with larger ligaments on the rim edge.

3.3. Dynamic behaviors of liquid jet at large flow rates

For large flow rates, liquid jets are formed, however, the dynamic behaviors are quite different from small flow rates. Microwaves emerge on the surface of liquid jet and the effect

of electric field is weakened for the hydrodynamic impact could not be ignored. The ethanol jet behaviors for five various flow rates without influence of electric field are shown in Figure 8 (a). As mentioned in section 3.1, the droplet frequency turns so fast with higher flow rates that the liquid bridge could not break off, forming a string of merging droplets. Therefore, the liquid injection turns into jet with surface waves. When electric field is exerted on the liquid jet, the breakup characteristics remain stable, which means the effect of electric field becomes weak compared with hydrodynamic impact. However, the film breakup regime appears at quite large Bo_E. The evolution process for ethanol jet exerted electric potential at Re=172 is illustrated In Figure 8 (b). As can be seen, the film breakup regime appears with Bo_E as high as 67, which could be assumed that the electric field has no effect on liquid jet while hydrodynamic is in priority.

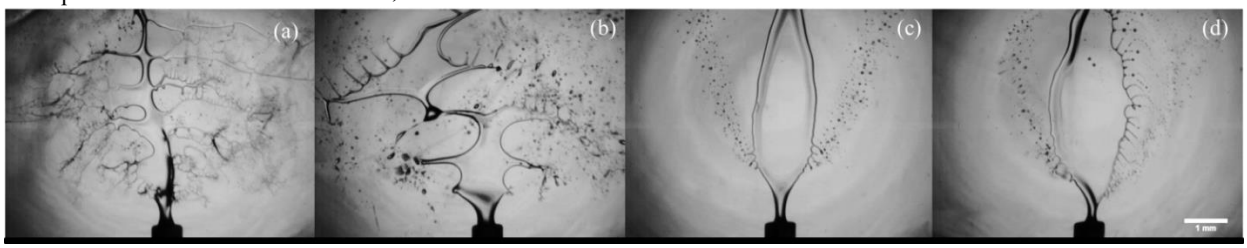

Figure 7. Various sheet breakup characteristics

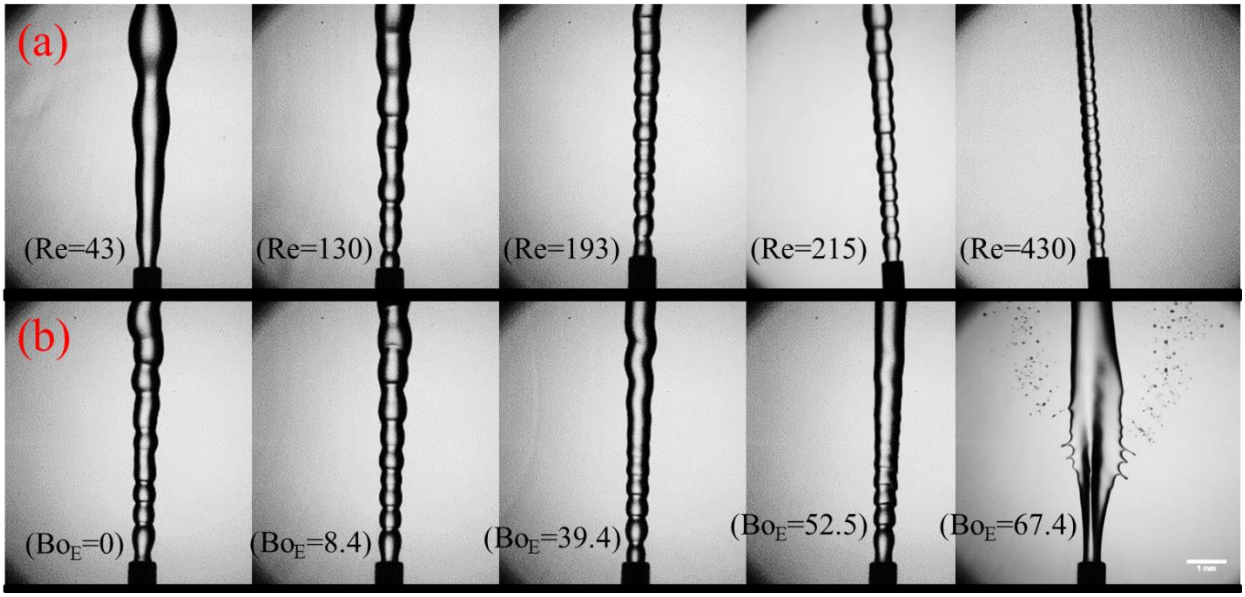

Figure 8. Ethanol jet dynamic behaviors. Group (a) Bo_E=0; Group (b) Re=172

From Figure 8, it can be seen that liquid jet has different characteristics with various Re and Bo_E. Liquid jet prevails for large Re and is stretched to be thin by electric stress for large Bo_E, fine droplets ejected from microwaves on the edge of jet surface. According to Rayleigh limit theory (Rayleigh, 1882) given by Eq. (5), Eq. (6) can be reached, which reveals that liquid could not obtain enough charges to reach Rayleigh limit with large flow rate. Thus, it's hard for electric stress to effectively affect jet behaviors at small Bo_E for more charges q are needed with large flow rate Q, according to Eq. (6).

$$q = 2\pi d\sqrt{2\varepsilon\sigma d} \tag{5}$$

$$q = 2\pi d\sqrt{2\varepsilon\sigma d} \tag{6}$$

In addition, the surface microwave length decreases with the increase of Re and Bo_E while surface microwave amount rises up. Figure 9 gives the surface wave length variation related to different Re and Bo_E. It can be seen that the wavelength decreases fast with the increase of Re while small declining trend and fluctuation are found with ascending Bo_E. In liquid jet process at large flow rates, hydrodynamic stress plays a significant role, instability of jet surface wave transits to turbulence, decreasing wave length. Although Bo_E has less effect on liquid jet, wave length is still reduced with increasing Bo_E.

What needs to be pointed out is that there exists a critical Re of 170 in this experiment, where electric field almost has

no effect on liquid jet injection. One of the reasons might be that large liquid volume needs more charges to deform, which is supported by the fact that much higher electric field could play a role in jet deformation behaviors. Another reason to explain this phenomenon could be that there is not enough time for liquid to be charged because of high flow rates. In other words, the liquid speed surpasses charge relaxation time so that liquid could not carry enough charges to deform. After critical *Re*, raising Bo_E is meaningless to enhance liquid dispersion as well as mass and heat transfer. This critical *Re* is obtained from the jet phase diagram with large *Re* as illustrated in Figure 10, which clearly shows that electric field is not suitable to exert on liquid dispersion for liquid jet behavior remains the same after *Re* = 170. It can be seen in Figure 10 that the above mentioned dynamic behaviors of single breakup regime and swing breakup regime at small flow rates disappears, a novel jet regime is observed with small exerted electric potential. Furthermore, the branch breakup regime shows up in small *Re* and Bo_E only, occupying smaller area in the jet phase diagram. Therefore, it could be inferred that jet regime and sheet regime are the main dynamic behaviors with large flow rates. With the rise of flow rates, sheet regime area becomes small and disappears at last.

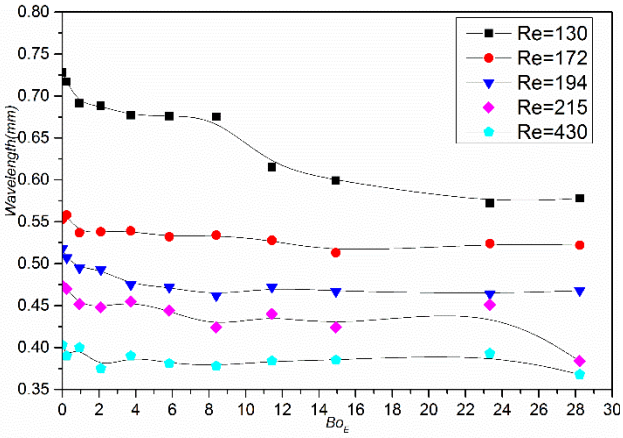

Figure 9. Jet surface wave length at various *Re* and Bo_E

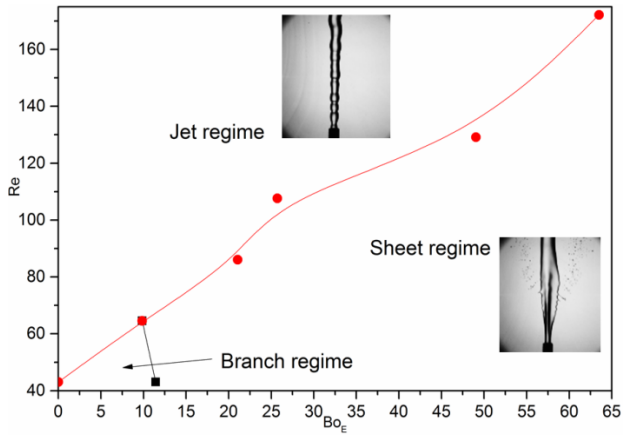

Figure 10. Ethanol jet phase diagram with large Re

4. Conclusion

In the present study, an experimental investigation is conducted to investigate the effect of electric field on the dynamic behavior of ethanol liquid injection surrounded by another immiscible soybean oil fluid. Two ethanol dispersion stages are distinguished based on the amount of *Re*. At small *Re*, four special droplet breakup regimes are illustrated in detail while the detailed droplet formation and breakup process are analyzed. Besides, the ethanol droplet breakup mechanisms are analyzed, which indicates that the increasing Bo_E decreases droplet size, resulting in the enhancement of interface heat and mass transfer. These results could be potential to develop novel liquid-liquid reactor with high efficiency. On the other hand, electric field has little effect on liquid jet injection for higher *Re*, while a critical *Re* of about 170 is obtained. And the liquid jet breakup regimes are different from small flow rates, jet regime and sheet regime are the main breakup regimes for high *Re*. With the effect of both electric and flow field, sheet breakup regime could be regarded as the optimal condition for charged liquid-liquid dispersion.

Acknowledgments

This work was supported by National Natural Science Foundation of China (Grant No. 51761145011; Postgraduate Research & Practice Innovation Program of Jiangsu Province (Grant No. KYCX17_1776).

References

Allan R.S., Mason S.G., 1962. Particle behavior in shear and electric fields I. Deformation and burst of fluid drops. Proceedings of Royal Society A 267 (1328): 45-61.

Coelho R., Debeau J., 1971. Properties of the tip-plane configuration, Journal of Physics D: Applied Physics 4 (9): 1266-1280.

Eastwood C.D., Armi L., Lasheras J.C., 2004. The breakup of immiscible fluids in turbulent flows. Journal of Fluid Mechanics 502: 309-333.

Eow J.S., Ghadiri M., Sharif A., 2003, Experimental studies of deformation and break-up of aqueous drops in high electric fields, Colloids and Surfaces A: Physicochemical and Engineering Aspects 225 (1): 193-210.

Feng J.Q., Scott T.C., 1996. A computational analysis of electrohydrodynamics of a leaky dielectric drop in an electric field. Journal of Fluid Mechanics 311: 289-326.

Gomez A., Tang K., 1994. Charge and fission of droplets in electrostatic sprays. Physics of Fluids 6 (1): 404-414.

Jalaal M., Khorshidi B., Esmaeilzadeh E., 2010. An experimental study on the motion, deformation and electrical charging of water drops falling in oil in the presence of high voltage D.C. electric field. Experimental Thermal and Fluid Science 34 (8): 1498-1506.

Jong-Wook H.A., and Seung-Man Yang., 2000. Deformation and breakup of Newtonian and non-Newtonian conducting drops in an electric field. Journal of Fluid Mechanics 405: 131-156.

Kim H.H., Kim J.H., Ogata A., 2011. Time-resolved high-speed camera observation of electrospray. Journal of Aerosol Science 42 (4): 249-263.

Kweon Y.C., Kim M.H., Cho H.J., Kang I.S., 1998. Study on the deformation and departure of a bubble attached to a wall in D.C./A.C. electric fields. International Journal of Multiphase Flow 24(1): 145-162.

Li Z.T., Li G.J., Huang H.B., Lu X.Y., 2011. Lattice Boltzmann study of electrohydrodynamic drop deformation with large density ratio. International Journal of Modern Physics C 22 (7): 29-744.

Marginean I., Nemes P., and Vertes A., 2006. Order-chaos-order transitions in electrosprays: The electrified dripping faucet. Physical Review Letters 97 (6): 064502.

Matsuyama T., Abe T., Yamamoto H., 2007. Lattice Boltzmann method study of Rayleigh instability of a charged droplet, Advanced Powder Technology 18(1): 93-104.

Min WL., An S., Na YK., Ju H.S., Huh J.Y., Kim H.Y., and Yoon S.S., 2013, Effects of pulsing frequency on characteristics of electrohydrodynamic inkjet using micro-Al and nano-Ag particles. Experimental Thermal & Fluid Science 46(46): 103-110.

Nemes P., Marginean I., Vertes A., 2007. Spraying mode effect on droplet formation and ion chemistry in electrosprays. Analytical Chemistry 79(8): 3105-3116.

Petera J., Strzelecki W., Agrawal D., 2005. Charged droplet and particle-mixing studies in liquid-liquid systems in the presence of non-linear electrical fields, Chemical Engineering Science 60 (1): 135-149.

Raisin J., Reboud J.L., Atten P., 2011. Electrically induced deformations of water–air and water–oil interfaces in relation with electro coalescence, Journal of Electrostatics 69(4): 275-283.

Rayleigh L., 1882. On the equilibrium of liquid conducting masses charged with electricity. The London, Edinburgh, and Dublin Philosophical Magazine and Journal of Science, 14(87): 184-186.

Reddy MN., Esmaeeli A., 2009. The EHD-driven fluid flow and deformation of a liquid jet by a transverse electric field. International Journal of Multiphase Flow 35(11): 1051-1065.

Reznik S.N., Yarin A.L., Theron A., and Zussman E., 2004, Transient and steady shapes of droplets attached to a surface in a strong electric field. Journal of Fluid Mechanics 516: 349-377.

Ristenpart W.D., Bird J.C., Belmonte A., Dollar F., Stone H.A., 2009. Non-coalescence of oppositely charged drops. Nature 461: 377-380.

Salipante P.F., Vlahovska P.M., 2010. Electrohydrodynamics of drops in strong uniform DC electric fields. Physics of Fluids 22(11): 111.

Seyed-Yagoobi J., Bryan J.E., 1999. Enhancement of heat transfer and mass transport in single-phase and two-phase flows with electrohydrodynamics. Advances in Heat Transfer 33: 95-186.

Jejurkar SY., Yadav G., Mishra D.P., 2017. Visualizations of sheet breakup of non-Newtonian gels loaded with nanoparticle, International Journal of Multiphase Flow 100: 57-76.

Taylor G.I., 1996, Studies in electrohydrodynamics: I. The circulation produced in a drop by an electric field, Proceedings of Royal Society A 291(1425): 159-167.

Vizika O., Saville D.A., 1992. The electrohydrodynamic deformation of drops suspended in liquids in steady and oscillatory electric fields. Journal of Fluid Mechanics 239: 1-21.

Wang Y., Tan M.K., Go D.B., Chang H.C., 2012. Electrospray cone-jet breakup and droplet production for electrolyte solutions. Europhysics Letters 100(2): 29901.

Wang D., Wang J., Wang X., Huo Y., Yongphet P., 2019a, Experimental investigation on the deformation and breakup of charged droplets in dielectric liquid medium. International Journal of Multiphase Flow, 114, 39-49.

Wang D., Wang J., Liu H., Huo Y., Hu W., 2019b, Reaction kinetics of waste cooking oil transesterification under electric field. Waste and Biomass Valorization https://doi.org/10.1007/s12649-019-00673-2.

Shin W.T., Yiacoumi S., 1997. Experiments on electrostatic dispersion of air in water. Industrial and Engineering Chemistry Research 36: 3647-3655.

